Density pattern in supercritical flow of liquid ^{4}He

F. Ancilotto,[1] F. Dalfovo,[2,3] L. P. Pitaevskii,[3,4] and F. Toigo[1]
[1]*INFM (Udr Padova and DEMOCRITOS National Simulation Center, Trieste, Italy) and Dipartimento di Fisica "G. Galilei," Università di Padova, via Marzolo 8, I-35131 Padova, Italy*
[2]*BEC-INFM, Istituto Nazionale per la Fisica della Materia, Trento, Italy*
[3]*Dipartimento di Fisica, Università di Trento, 38050 Povo, Italy*
[4]*Kapitza Institute for Physical Problems, ul. Kosygina 2, 117334 Moscow, Russia*
(Received 30 November 2004; revised manuscript received 25 January 2005; published 31 March 2005)

A density-functional theory is used to investigate the instability arising in superfluid ^{4}He as it flows at velocity u just above the Landau critical velocity of rotons v_c. Confirming an early theoretical prediction by one of us [JETP Lett. **39**, 511 (1984)], we find that a stationary periodic modulation of the density occurs, with amplitude proportional to $(u-v_c)^{1/2}$ and wave vector equal to the roton wave vector. This density pattern is studied for supercritical flow both in bulk helium and in a channel of nanometer cross section.

DOI: 10.1103/PhysRevB.71.104530 PACS number(s): 67.90.+z, 67.40.Hf

I. INTRODUCTION

According to the Landau criterion, superfluid motion of ^{4}He moving with velocity u is possible only if $u<v_c$, where the critical velocity v_c is equal to the slope of the tangent to the roton part of the spectrum ($v_c \sim 56$ m/s). As the Landau critical velocity v_c is reached, the liquid becomes unstable against a spontaneous excitation of rotons. Reaching the roton critical velocity is difficult in practice since other types of excitations, e.g., quantized vortices, are produced in bulk ^{4}He well below v_c. However, the occurrence of vorticity could be suppressed by allowing ^{4}He to flow through very narrow channels. In fact, the critical velocity for the creation of vortex pairs in a channel of diameter D is $v_c^{vortex} \sim (\hbar/MD)\ln(D/\xi)$,[1] where ξ is the ^{4}He healing length ($\xi \sim 1$ Å), so that it can exceed the roton critical velocity for channels of nanometer size.[2]

Several years ago, a theoretical prediction was made by one of us[3] that superfluid ^{4}He flowing at a velocity greater than the Landau critical velocity v_c should undergo a phase transition from a spatially homogeneous state to a layered state characterized by a periodic density modulation in the direction of motion. Such a modulation is stationary in the frame moving with the fluid and has a characteristic wavelength $\lambda = 2\pi\hbar/p_c \sim 3.58$ Å, where p_c is the roton momentum. This prediction was derived within a simplified model describing a weakly interacting roton gas with coupling constant g. The nature of the transition was found to depend on the sign of g: if $g>0$ ($g<0$), the transition is predicted to be continuous (discontinuous). In Ref. 3, the estimate $g = 2 \times 10^{-38}$ erg cm^3 (Ref. 4) was used and the amplitude of the density modulations was found to be[5]

$$\frac{\Delta\rho}{\rho_0} = 2\left(\frac{|A|^2(u-v_c)p_c}{\rho_0 g}\right)^{1/2}, \tag{1}$$

where ρ_0 is the bulk density and $|A|^2\delta(\hbar\omega - \epsilon(p_c))$ is the roton contribution to the dynamic structure factor $S(q,\omega)$. In Ref. 3, the latter was estimated by ignoring the multiphonon part of $S(q,\omega)$ and using the f-sum rule. A better estimate can be extracted from neutron scattering experiments,[6] where one finds $|A|^2 \simeq 0.9$. Inserting this value in Eq. (1), one gets

$$\Delta\rho/\rho_0 \simeq 3[(u-v_c)/v_c]^{1/2}. \tag{2}$$

The occurrence of this stationary nonuniform state originates from the presence of a pronounced minimum at $p=p_c$ in the bulk ^{4}He spectrum, $\epsilon(p)$, and is similar to the structural phase transition in crystals induced by the softening of phonon frequencies with some defined wavelength. In the numerical simulations of Ref. 7, similar density patterns were found in superfluid ^{4}He as a result of roton emission by a moving ion, when the ion velocity exceeds v_c. In the present work, we systematically investigate this type of stationary density modulations by means of density-functional (DF) calculations. We consider the uniform flow in bulk liquid (with no vorticity) as well as in a nanochannel and we compare our numerical results with the analytic predictions of Ref. 3.

II. DENSITY FUNCTIONAL

We use the DF approach proposed in Ref. 8 and later improved in Ref. 9, which gives a quite accurate description of inhomogeneous configurations of liquid ^{4}He at $T=0$. The energy of the system is expressed as

$$E_0[\rho] = E_c[\rho] + \frac{\hbar^2}{2M}\int d\mathbf{r}(\boldsymbol{\nabla}\sqrt{\rho})^2. \tag{3}$$

The explicit form of the energy functional E_c is given in the Appendix. The *static* equilibrium profile $\rho(\mathbf{r})$ in an arbitrary external potential can be obtained by minimizing the functional $E_0[\rho]$ with respect to density variations, subject to the constraint of a constant number of atoms. The *dynamics* can be studied as well by means of the time-dependent DF method, with the DF proposed in Ref. 9 playing the role of the effective Hamiltonian driving the time evolution of the system. In the dynamical case, the functional contains an explicit dependence upon the local current density field $\mathbf{j}(\mathbf{r})$ through a phenomenological term which accounts not only

for the usual hydrodynamic current density but also for nonlocal "backflow" effects. The resulting DF (called the Orsay-Trento functional), which will be used in our calculations, can be written as

$$E[\rho,\mathbf{v}] = E_0[\rho] + \int d\mathbf{r} H_J. \tag{4}$$

Its explicit form is given in the Appendix. An appealing feature of the above functional, which turns out to be essential to perform accurate time-dependent DF calculations,[9,10] is that is reproduces quantitatively not only a number of static properties, but also the observed phonon-roton spectrum of bulk ^{4}He.

The minimization of the above density-current functional, subject to the constraint of a fixed number of ^{4}He atoms and of fixed total momentum, can be done in practice by evolving in the imaginary time domain a nonlinear Schrödinger equation for the order parameter $\Psi(\mathbf{r})$, where the Hamiltonian operator is given by $H=-\hbar^2/(2M)\nabla^2+U[\rho,\mathbf{v}]$. The effective potential U is defined in terms of the variational derivative of the energy functional, and its explicit expression can be found in the Appendix. From the knowledge of the complex wave function $\Psi \equiv \phi e^{i\Theta}$ one can get immediately the density $\rho(\mathbf{r})=\phi^2$ and the velocity field $\mathbf{v}(\mathbf{r}) = (\hbar/M)\nabla\Theta$. Since we are interested in stationary states of ^{4}He in the presence of a uniform flow, we minimize the above functional in the frame of reference moving with the liquid, which we assume to flow with some given velocity u along the x axis: The Hamiltonian density H thus acquires an additional term $H'=H-u\hat{P}_x$, $\hat{P}_x$ being the ^{4}He total momentum component along the direction of motion.

III. BULK LIQUID

First, we address the problem of the Landau roton instability in bulk. As discussed above, we expect that when $u > v_c$, the uniform density configuration is not stable, but it is instead a metastable state corresponding to a saddle point of the energy landscape of ^{4}He. In our case, the system is allowed to reach the lowest energy configuration by following the (dissipative) imaginary-time evolution. The calculation is performed in a periodically repeated supercell where the size of the cell along the x direction (which we take as the direction of ^{4}He motion) is L. Our procedure to trigger the instability is the following: we start with the uniform system in the moving frame of reference and slightly perturb the (uniform) density with a sinusoidal modulation with a small arbitrary amplitude and with a wavelength λ allowed by the periodic boundary conditions in L. We then minimize the functional in the frame of reference moving with some chosen velocity u, with the only constraint of a constant number of ^{4}He atoms. If L or λ are not a multiple of the characteristic wavelength $\lambda_c \equiv (2\pi)/k_c$ ($k_c \equiv p_c/\hbar$ being the Landau critical wave vector), then, irrespective of the initial perturbation and of the particular value chosen for u, the perturbing modulation rapidly smoothes out during the minimization, and the uniform liquid state is recovered as the minimum energy configuration.

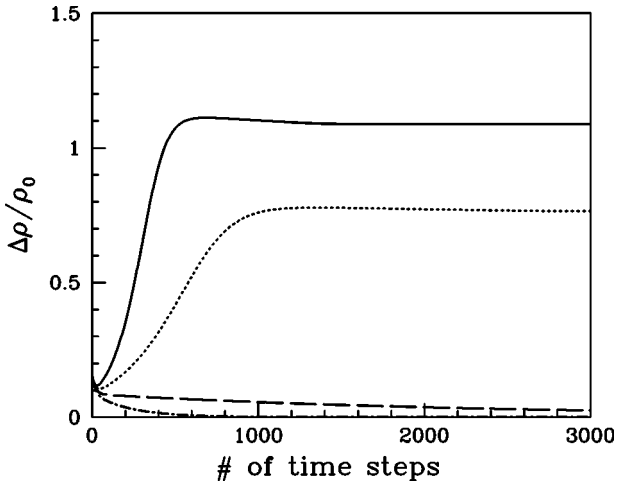

FIG. 1. Amplitude of the density modulation along the direction of ^{4}He motion, computed during the functional minimization. Solid line: $u=1.29v_c$, dotted line: $u=1.14v_c$, dashed line: $u=0.99v_c$, dash-dot line: $u=0.84v_c$.

The Landau instability shows up when the size of the cell is such to accommodate an integer number of characteristic wavelengths ($L=7\lambda_c$). In this case, we indeed find that there exists a threshold velocity v_c separating two regimes. If $u > v_c$, the stationary state is characterized by a density with a periodic modulation of wavelength λ_c and with an amplitude depending on u. On the contrary, when $u < v_c$ the initial modulation is rapidly smeared out during the minimization, and again one finds that the density of the stationary state is uniform. The critical velocity is found to be $v_c \sim 58$ m/s, which coincides with the minimum value of $\epsilon(p)/p$ predicted by the same DF and is also very close to the value of the Landau critical velocity of rotons as obtained from the experimental phonon-roton spectrum. This behavior is summarized in Fig. 1, where we plot the evolution of the amplitude of the density modulation as it varies during the minimization procedure, for four different ^{4}He velocities: the two upper lines have $u > v_c$, whereas the two lower lines have $u < v_c$. Note the critical slowing down for values of the ^{4}He velocity close to the critical value v_c, where a very long imaginary-time evolution is required to converge towards the equilibrium stationary state.

Different stationary density profiles along the direction of ^{4}He motion, corresponding to different values of $u > v_c$, are shown in Fig. 2. The average value of each curve corresponds to the saturation density of bulk ^{4}He, $\rho_0 = 0.0218$ Å^{-3}. A fit to the calculated points shows that their shapes, at least for values of u not too large, are almost exactly sinusoidal, i.e., $\rho(x)=\rho_0[1+(\Delta\rho/\rho_0)\sin(k_c x)]$. In Fig. 3, we also show the x component of the calculated ^{4}He velocity $\mathbf{v}(\mathbf{r})=(\hbar/M)\nabla\Theta$, in units of v_c, for the same states of Fig. 2. Note the oscillating character of the velocity, in phase with the density modulation, and the large amplitude of oscillations, which becomes more asymmetric as the velocity increases. The spatial average of the velocity profiles shown in Fig. 3 is zero, as expected.

The main result of this work is summarized in Fig. 4, where we show the behavior of the amplitude $\Delta\rho/\rho_0$ for u

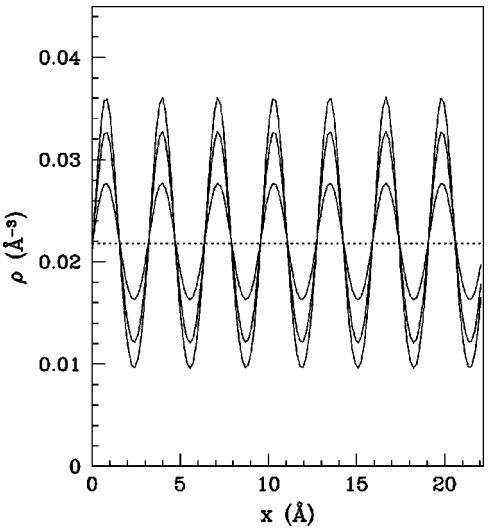

FIG. 2. Density profiles along the direction of ^{4}He flow x axis. The three profiles have been calculated, in order of increasing amplitude, with $u=1.07$, 1.22, and 1.37 v_c, respectively.

$>v_c$. We find that the law $\Delta\rho/\rho_0=1.01[(u-v_c)/v_c]^{1/2}$ (solid line) very nicely fits the numerical results (points). The velocity dependence is thus the same as in Eq. (2) except for the different numerical coefficient. Our DF calculations are consistent with a repulsive (positive g) roton-roton interaction. Using Eq. (1) and the fitting coefficient 1.01, we find $g\simeq 1.8\times 10^{-37}$ erg cm^3. It is worth stressing that direct measurements of g are not available and previous theoretical estimates significantly differ both in magnitude and sign (see, for instance, Refs. 12,13, and references therein).

IV. FLOW IN A NARROW CHANNEL

Now we investigate the motion of liquid ^{4}He in a narrow channel of nanometer transverse dimensions. We consider

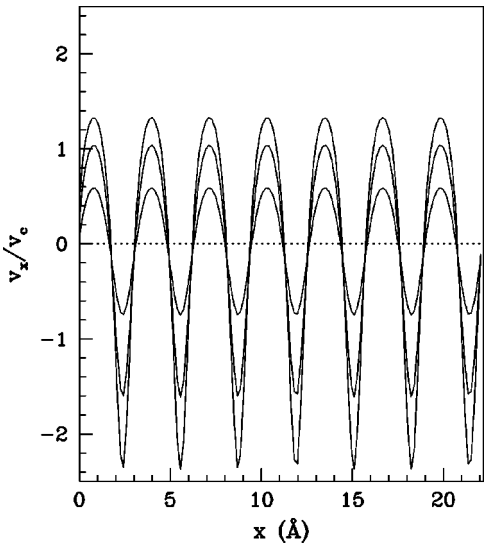

FIG. 3. Velocity profile along the direction of ^{4}He flow x axis. Same values of u as in Fig. 2.

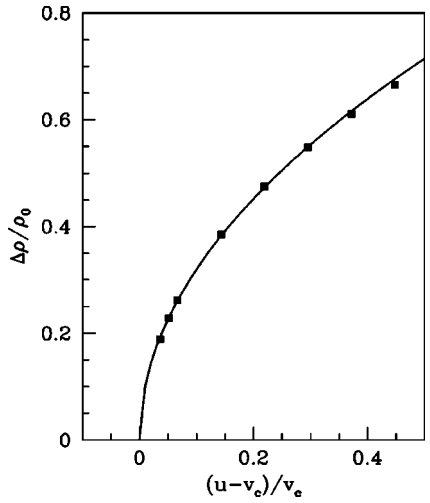

FIG. 4. Amplitude of the density modulation as a function of the fluid velocity. Points: DF results. Line: fitting function 1.01 $[(u-v_c)/v_c]^{1/2}$.

liquid ^{4}He confined between two infinitely extended, weakly attractive planar surfaces separated by a very small distance, $\sim$50 Å. We model the two surfaces with an external potential which mimics the adsorption properties of the Rb surface, which is the weakest surface which is wet at $T=0$ by liquid ^{4}He.[11] The number of ^{4}He atoms in the system is chosen in such a way that, when the ^{4}He is at rest, the equilibrium density near the center of the channel reaches the value corresponding to the saturation density of bulk ^{4}He, ρ_0.

In Fig. 5, we show the density profile along the z direction, i.e., across the channel, for $u=0$. The ^{4}He density decreases rapidly to zero near the solid surfaces on both sides of the channel due to the ^{4}He-Rb interaction. The same interaction is also responsible for the density oscillations near the walls. The dotted line shows the value of the bulk saturation density ρ_0. Figure 6 shows a contour plot of the density in the xz plane for the stationary state developed at $u=1.22v_c$. The complex pattern near the walls is again due to

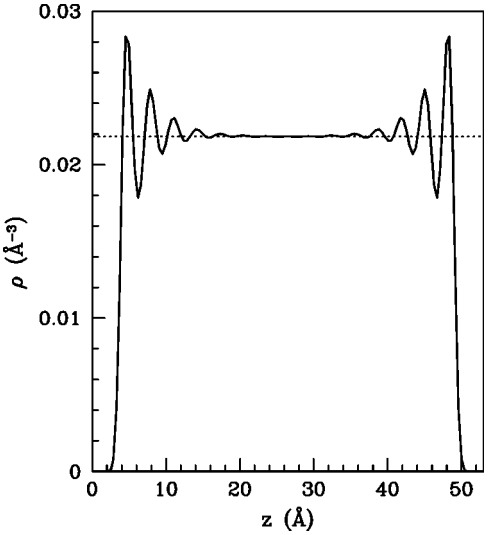

FIG. 5. Density profile across the channel section.

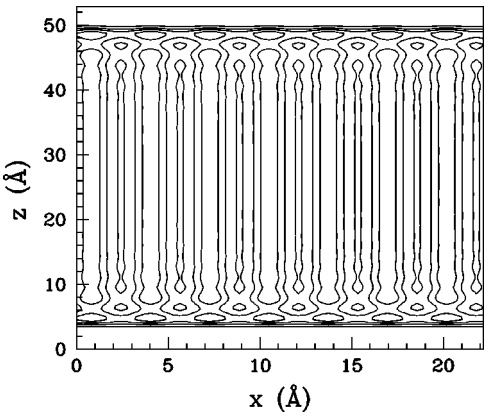

FIG. 6. Contour plots of the density along the channel.

the ^{4}He-Rb interaction. However, the dominant feature is the density modulation along x in the central part of the channel. This sinusoidal oscillation coincides, for the same value of u, with the one that we already obtained in bulk ^{4}He.

It is worth noticing that the DF theory could also be applied to the case of larger velocity, $u \gg v_c$, where one expects the occurrence of solitonlike structures, analogous to the nonlinear waves discussed in Refs. 14,15 for weakly interacting Bose gases. In this limit, however, one should take care of possible mechanisms of dynamical instability. This problem cannot be addressed within our stationary DF approach and remains open. Nevertheless, it is reasonable to believe that the density pattern found in the present work can be unstable at large amplitude in bulk helium, but stable in sufficiently narrow channels.

V. CONCLUSIONS

Our DF calculations support the predictions of Ref. 3 on the occurrence of a density pattern in the supercritical flow just above v_c and in the absence of vorticity. Due to the short wavelength of the density modulations, of the order of the atomic spacing, its direct observation, with x rays for instance, might be difficult. Indirect evidence of the density modulations could, however, be measurable, for example through their possible effects on transport properties. Recently, He adsorption within a regular porous medium called FSM-16 has been studied.[16] This silica-based material is characterized by ordered arrays of long, uniform pores, with diameters ranging from 1.5 to 10 nm. When ^{4}He is adsorbed within the pores, one to two solidlike layers are expected to form, coating the internal walls of the pores, leaving, however, room for additional ^{4}He in the liquid state. A pressure gradient between two open ends of an array of pores could in principle be used to force liquid ^{4}He to move through this system, until it is expelled from the pore end. If during this process the critical velocity is reached, then the occurrence of the above described density pattern might induce the fragmentation of the ejected liquid filament into regularly distributed nanodroplets. A similar process might occur in the experiments of Ref. 17, where liquid ^{4}He is discharged into vacuum through a micrometer nozzle. The structure of the ejected filament was interpreted in terms of a Rayleigh instability, but the occurrence of density patterns near the nozzle could also play a role.[18] In this perspective, the effects of density modulations in ^{4}He supercritical flow in this type of experiments deserve further investigations. Finally, it is worth mentioning that a similar phenomenon may occur in Bose-Einstein condensed gases with dipole-dipole interactions.[19]

ACKNOWLEDGMENTS

We thank Maurizio Rossi for useful conversations. One of us (F.D.) would like to thank the Dipartimento di Matematica e Fisica dell'Università Cattolica del Sacro Cuore, Brescia, where part of this work was done.

APPENDIX

In this work, we use the Orsay-Trento density functional as defined in Ref. 9. The energy E_c in Eq. (3) has the form

$$E_c[\rho] = \frac{1}{2}\int d\mathbf{r}\int d\mathbf{r}'\rho(\mathbf{r})\rho(\mathbf{r}')V_\ell(|\mathbf{r}-\mathbf{r}'|) + \frac{c_2}{2}\int d\mathbf{r}\rho(\mathbf{r}) \times(\overline{\rho_{\mathbf{r}}})^2 + \frac{c_3}{3}\int d\mathbf{r}\rho(\mathbf{r})(\overline{\rho_{\mathbf{r}}})^3 + \frac{\hbar^2}{4M}\alpha_s\int d\mathbf{r}\int d\mathbf{r}' F \times(\mathbf{r}-\mathbf{r}')\left(1-\frac{\rho(\mathbf{r})}{\rho_{0s}}\right)\times\ \nabla\rho(\mathbf{r})\,\nabla\rho(\mathbf{r}')\left(1-\frac{\rho(\mathbf{r}')}{\rho_{0s}}\right). \tag{A1}$$

Here $\rho(\mathbf{r})$ is the density of liquid ^{4}He and M is its atomic mass. The first term contains a Lennard-Jones He-He pair potential $V_\ell(r)$ screened at distances shorter than a characteristic length h_ℓ. In the second and the third terms, the weighted density $\overline{\rho}$ is the average of the density over a sphere of radius h_ℓ, that is, $\overline{\rho_r} \equiv \int d\mathbf{r}'\rho(\mathbf{r}')\Pi_h(|\mathbf{r}-\mathbf{r}'|)$, with $\Pi_h(r) = 3/(4\pi h^3)$ when $r<h$ and $\Pi_h(r)=0$ otherwise. These terms account for the internal kinetic energy and for the increasing contribution of the hard-core He-He repulsion when the density is increased. The last term contains the gradient of the density at different points and corresponds to a nonlocal correction to the kinetic energy. The free parameters h_ℓ, c_2, c_3 are adjusted in order to reproduce the experimental values of the density, of the energy per atom, and of the compressibility for bulk liquid ^{4}He at zero pressure, while the width of the Gaussian function F and the parameter α_s are fixed to reproduce the peak of the static response function in bulk liquid. The parameter ρ_{0s} is finally fixed to ensure an accurate pressure dependence of the response function. A detailed description of the various terms and the numerical values of the parameters can be found in Ref. 9.

The term H_J appearing in Eq. (4) is given by

$$H_J[\rho,\mathbf{v}] = \frac{\rho(\mathbf{r})}{2}M\mathbf{v}(\mathbf{r})^2 - \frac{M}{4}\int d\mathbf{r}' V_J(|\mathbf{r}-\mathbf{r}'|)\rho(\mathbf{r})\rho(\mathbf{r}') \times[\mathbf{v}(\mathbf{r})-\mathbf{v}(\mathbf{r}')]^2, \tag{A2}$$

where the first term is the usual hydrodynamic current density, while the second term accounts in a phenomenological way for nonlocal effects due to the "backflow" current density.[9]

Finally, the effective potential U entering the Hamiltonian operator for ^{4}He (see text) can be readily evaluated by functional differentiation of the energy functional (4) and it reads

$$U[\rho,\mathbf{v}] = \int d\mathbf{r}'\rho(\mathbf{r}')V_\ell(|\mathbf{r}-\mathbf{r}'|) + \frac{c_2}{2}\overline{\rho}(\mathbf{r})^2 + \frac{c_3}{3}\overline{\rho}(\mathbf{r})^3 + \int d\mathbf{r}'\rho(\mathbf{r}')[c_2\Pi_h(|\mathbf{r}-\mathbf{r}'|)\overline{\rho}(\mathbf{r}')$$
$$+ c_3\Pi_h(|\mathbf{r}-\mathbf{r}'|)\overline{\rho^2}(\mathbf{r}')] + \frac{\alpha_s}{2M}\left(1-\frac{\rho(\mathbf{r})}{\rho_0}\right)\int d\mathbf{r}'\left(1-\frac{\rho(\mathbf{r}')}{\rho_0}\right)\boldsymbol{\nabla}_{r'}\rho(\mathbf{r}')\cdot\boldsymbol{\nabla}_r F(|\mathbf{r}'-\mathbf{r}|)$$
$$- \frac{M}{2}\int d\mathbf{r}' V_J(|\mathbf{r}-\mathbf{r}'|)\rho(\mathbf{r}',t)[v(\mathbf{r})-v(\mathbf{r}')]^2 + \frac{i}{2\rho(\mathbf{r})}\boldsymbol{\nabla}\cdot\int d\mathbf{r}' V_J(|\mathbf{r}-\mathbf{r}'|)\rho(\mathbf{r})\rho(\mathbf{r}')[\mathbf{v}(\mathbf{r})-\mathbf{v}(\mathbf{r}')]. \quad \text{(A3)}$$

[1] R. P. Feynman, in *Progress in Low Temperature Physics* (North Holland, Amsterdam, 1955), Vol. 1, p. 17.

[2] In this geometry, the problem is similar to that of elongated Bose-Einstein condensates in dilute gases, where dissipation effects can originate either from vortex states or from Bogoliubov excitations. Seè, for instance, C. Raman, M. Kohl, R. Onofrio, D. S. Durfee, C. E. Kuklewicz, Z. Hadzibabic, and W. Ketterle, Phys. Rev. Lett. **83**, 2502 (1999) and P. O. Fedichev and G. V. Shlyapnikov, Phys. Rev. A **63**, 045601 (2001).

[3] L. P. Pitaevskii, JETP Lett. **39**, 511 (1984).

[4] A. J. Smith, R. A. Cowley, A. D. B. Woods, W. G. Stirling, and P. Martel, J. Phys. C **10**, 543 (1977).

[5] We note on passing that the factor 2 was erroneously missing in Ref. 3.

[6] R. A. Cowley and A. D. B. Woods, Can. J. Phys. **49**, 177 (1971).

[7] N. G. Berloff and P. H. Roberts, Phys. Lett. A **274**, 69 (2000).

[8] J. Dupont-Roc, M. Himbert, N. Pavloff, and J. Treiner, J. Low Temp. Phys. **81**, 31 (1990).

[9] F. Dalfovo, A. Lastri, L. Pricaupenko, S. Stringari, and J. Treiner, Phys. Rev. B **52**, 1193 (1995).

[10] L. Giacomazzi, F. Toigo, and F. Ancilotto, Phys. Rev. B **67**, 104501 (2003).

[11] F. Ancilotto, F. Faccin, and F. Toigo, Phys. Rev. B **62**, 17 035 (2000).

[12] K. Nagai and F. Iwamoto, Prog. Theor. Phys. **85**, 169 (1991).

[13] F. Pistolesi, Phys. Rev. Lett. **81**, 397 (1998); J. Low Temp. Phys. **113**, 597 (1998).

[14] V. Hakim, Phys. Rev. E **55**, 2835 (1997).

[15] N. Pavloff, Phys. Rev. A **66**, 013610 (2002).

[16] H. Ikegami, T. Okuno, Y. Yamato, J. Taniguchi, N. Wada, S. Inagaki, and Y. Fukushima, Phys. Rev. B **68**, 092501 (2003).

[17] R. E. Grisenti and J. P. Toennies, Phys. Rev. Lett. **90**, 234501 (2003).

[18] M. Rossi, Laurea thesis.

[19] L. Santos, G. V. Shlyapnikov, and M. Lewenstein, Phys. Rev. Lett. **90**, 250403 (2003); S. Giovanazzi and D. H. J. O'Dell, Eur. Phys. J. D **31**, 439 (2004).